Mechanics and Materials Center
TEXAS A&M UNIVERSITY
College Station, Texas

AD-A225 790

ANALYSIS OF DAMAGE GROWTH IN PARTICULATE COMPOSITES
USING A WORK POTENTIAL

TECHNICAL REPORT

R.A. SCHAPERY

MM 27010-90-10

AUGUST 1990

90 08 22 080

REPORT DOCUMENTATION PAGE

1a. REPORT SECURITY CLASSIFICATION unclassified	1b. RESTRICTIVE MARKINGS
2a. SECURITY CLASSIFICATION AUTHORITY	3. DISTRIBUTION/AVAILABILITY OF REPORT
2b. DECLASSIFICATION/DOWNGRADING SCHEDULE	
4. PERFORMING ORGANIZATION REPORT NUMBER(S) MM-27010-90-10	5. MONITORING ORGANIZATION REPORT NUMBER(S)

6a. NAME OF PERFORMING ORGANIZATION Mechanics & Materials Center Civil Engineering Department	6b. OFFICE SYMBOL (If applicable)	7a. NAME OF MONITORING ORGANIZATION ONR
6c. ADDRESS (City, State and ZIP Code) Texas A&M University College Station, Texas 77843		7b. ADDRESS (City, State and ZIP Code)

8a. NAME OF FUNDING/SPONSORING ORGANIZATION Department of the Navy	8b. OFFICE SYMBOL (If applicable)	9. PROCUREMENT INSTRUMENT IDENTIFICATION NUMBER Grant No. N00014-89-J-3012

8c. ADDRESS (City, State and ZIP Code) Office of the Chief of Naval Research 800 N. Quincy Street Arlington, VA 22217-5000	10. SOURCE OF FUNDING NOS.			
	PROGRAM ELEMENT NO.	PROJECT NO.	TASK NO.	WORK UNIT NO.
11. TITLE (Include Security Classification) Analysis of Damage Growth in Particulate Composites Using a Work Potential				

12. PERSONAL AUTHOR(S)
R.A. Schapery

13a. TYPE OF REPORT Technical	13b. TIME COVERED FROM _____ TO _____	14. DATE OF REPORT (Yr., Mo., Day) August 1990	15. PAGE COUNT 10

16. SUPPLEMENTARY NOTATION

17.	COSATI CODES		18. SUBJECT TERMS (Continue on reverse if necessary and identify by block number)
FIELD	GROUP	SUB. GR.	Particulate Composites Rubber Damage Continuum Damage Mechanics Micromechanics

19. ABSTRACT (Continue on reverse if necessary and identify by block number)

The elements of a theory for elastic composites with a changing microstructure, such as microcracking, are reviewed. This formulation, which uses internal state variables and potentials like strain energy and work, is then illustrated by mathematically characterizing and predicting the damage and deformation behavior of particle-filled rubber under axial straining and confining pressure. Next, a micromechanical model, which accounts for effects of distributed microcracks and particles on overall deformation behavior, is described and shown to be in agreement with experimental findings. It is then indicated how this model may be combined with the potential theory to extend the results from specimens under axial straining and pressure to more general strain states.

20. DISTRIBUTION/AVAILABILITY OF ABSTRACT UNCLASSIFIED/UNLIMITED ☐ SAME AS RPT. ☐ DTIC USERS ☐	21. ABSTRACT SECURITY CLASSIFICATION

22a. NAME OF RESPONSIBLE INDIVIDUAL Dr. Richard S. Miller, Code 1132P	22b. TELEPHONE NUMBER (Include Area Code) (202) 696-4405	22c. OFFICE SYMBOL

DD FORM 1473, 83 APR   EDITION OF 1 JAN 73 IS OBSOLETE.

ANALYSIS OF DAMAGE GROWTH IN PARTICULATE COMPOSITES

USING A WORK POTENTIAL*

R.A. Schapery
Department of Civil Engineering
Texas A & M University
College Station, Texas 77843

Address effective September 1, 1990: Department of Aerospace
Engineering and Engineering Mechanics,
The University of Texas, Austin, Texas 78712

ABSTRACT

The elements of a theory for elastic composites with a changing microstructure, such as microcracking, are reviewed. This formulation, which uses internal state variables and potentials like strain energy and work, is then illustrated by mathematically characterizing and predicting the damage and deformation behavior of particle-filled rubber under axial straining and confining pressure. Next, a micromechanical model, which accounts for effects of distributed microcracks and particles on overall deformation behavior, is described and shown to be in agreement with experimental findings. It is then indicated how this model may be combined with the potential theory to extend the results from specimens under axial straining and pressure to more general strain states.

NOMENCLATURE

a, b, R	Radii in model composite
A_{ij}, B_{ij}	Moduli
c_{ij}	Coefficients in dual energy
E	Young's modulus GPa (lb/in^2)
f_m	Thermodynamic force
p	Pressure GPa (lb/in^2)
q_j	Generalized displacement
Q_j	Generalized force
S, S_m	Structural parameters
u_j	Displacement
v, e_d	Dilatation
V, V_o	Volume
W	Strain energy
W_T, W_{TD}	Total work and dual work
ε	Strain
ν	Poisson's ratio
σ	Stress

1. INTRODUCTION

In this paper we use a theory based on thermodynamics with internal state variables (Schapery, 1990a) to characterize and then predict mechanical behavior of a highly-filled rubber with distributed microcracks. A similar study of fiber-reinforced plastic is reported elsewhere (Schapery, 1989a). The previously developed micromechanical model (Schapery, 1986) serves to guide the thermodynamic formulation for general stress states and to identify the physical significance of the internal state variables. The effect of individual particles and microcracks is smeared out in that the composite is represented as a homogeneous continuum on a scale that is much larger than particle and crack sizes. This type of idealization is basic to the many studies in "continuum damage mechanics"; see, e.g. Krajcinovic and Lemaitre (1987). However, the underlying thermodynamic formulation (Schapery, 1990a) is not limited to this idealization.

The nonlinear behavior of filled rubber, such as solid propellant, tires and numerous other commercial rubber products, has been studied extensively over many years. Large strains (Swanson, 1983), vacuole (or crack) formation and growth (Farris, 1968), viscoelasticity (Schapery, 1982), and the Mullins' effect in unloading behavior (Mullins, 1969) all contribute to the complex behavior of solid propellant, which is the material that is used here to illustrate the damage theory. In this paper we account for only nonlinearity of stress-strain behavior during loading. Viscoelasticity and the Mullins' effect may be incorporated using the approach described in other papers (Schapery, 1982, 1990a). In contrast to plasticity theory, nonlinear behavior during loading is <u>not</u> necessarily tied to residual (plastic) strains or other behavior associated with unloading; this point is illustrated by Schapery (1989a) for fibrous composites.

In Section 2 we summarize the primary results from the thermodynamic theory (Schapery, 1990a) which is expressed in terms of an arbitrary number of independent generalized displacements and internal state variables. Characterization of the behavior of solid propellant subjected to confining pressure and

---

axial stretching serves in Section 3 to illustrate the theory when one internal state variable is sufficient to account for the damage. An elementary model of microcracking is used in Section 4 to connect the internal state variables to the microstructure. It should be noted that Sections 3 and 4 describe and expand upon earlier work by Schapery (1986, 1987a). In Section 5 this model is used to generalize results for axisymmetric loading to a general strain state.

2. ELASTIC BEHAVIOR WITH CHANGING MICROSTRUCTURE

We consider an elastic structure or material whose thermodynamic state is a function of independent generalized displacements $q_j(j = 1,2,....J)$ and internal state variables $S_m(m = 1,2,...M)$ as well as temperature or entropy; inelastic behavior arises from changes in the S_m. Generalized forces Q_j are defined in the usual way in that

$$\delta W' = Q_j \delta q_j \quad \text{(j not summed)} \qquad (1)$$

for each virtual displacement δq_j, where δW is the virtual work. Then, from thermodynamics

$$Q_j = \partial W/\partial q_j \qquad (2)$$

where W is the Helmholtz free energy (when temperature is used as an independent state variable) or the internal energy (when entropy, instead of temperature, is an independent variable). For brevity, thermal effects will not be considered here, and therefore we shall refer to W simply as the strain energy. The generalized displacements q_j may be, for example, the uniform strains in a material element and Q_j the conjugate stresses, or q_j and Q_j may be, respectively, the displacements and forces applied to a structure.

The internal state variables serve to define changes in the structure such as micro- or macro-cracking, and are called structural parameters. Whenever any one $S_m \neq 0$, we specify as the evolution law,

$$f_m = \partial W_s/\partial S_m \qquad (3)$$

where $W_s = W_s(S_m)$ is a state function of one or more S_m; also, f_m is the thermodynamic force,

$$f_m = -\partial W/\partial S_m \qquad (4)$$

The left side of equation (3) is the available force for producing changes in S_m, while the right side is the required force. For any specific set of processes (i.e. histories $q_j(t)$), equation (3) may not be satisfied by some of the parameters; if it is not, those S_m will be constant. The subscript r or p will henceforth be used in place of m to designate parameters that change, which are taken to be R in number.

The total work done on the body by Q_j during an actual process (i.e., a process for which parameters change in accordance with equation (3)), starting at some reference state, is denoted by W_T,

$$W_T = \int Q_j dq_j \qquad (5)$$

where the summation convention for repeated indices is used. From equations (2)-(5) we find that W_T is a function of the state (q_j, S_m), and is given by

$$W_T = W + W_s \qquad (6)$$

where $W = W_s = 0$ in the reference state. Thus, W_s may be interpreted as that portion of the total work W_T which contributes to changes in the structure.

The second law of thermodynamics provides an inequality as a constraint on the changes in state,

$$\dot{W}_s = T S' \geq 0 \qquad (7)$$

where T is absolute temperature and S' is the entropy production rate. Even if equation (3) is satisfied for any one S_r, this inequality may not allow it to change. Additionally, instantaneous values of the S_r are such that they minimize the total work when the body passes through stable states; i.e.,

$$\partial W_T/\partial S_r = 0 \qquad (8)$$

$$(\partial^2 W_T/\partial S_r \partial S_p)\delta S_r \delta S_p > 0 \quad \text{if} \quad \delta S_r \delta S_r > 0 \qquad (9)$$

It should be emphasized that minimum total work is a necessary and sufficient condition for stability. In contrast, minimum W, rather than W_T, is equivalent to the stability condition for systems in the neighborhood of equilibrium states, according to classical thermodynamic theory. When $\dot{S}_m \neq 0$ and equation (3), with $f_m \neq 0$, governs changes in S_m, the system is not in the neighborhood of equilibrium; regardless of how slowly processes occur, the total entropy production W_s/T between any two states is the same.

It is observed that equation (3) represents R equations for finding the S_r as functions of q_j. Then, $W_T = W_T(q_j, S_r(q_j), S_q)$ where the S_q are the constant parameters. From equation (5),

$$Q_j = \partial W_T/\partial q_j \qquad (10)$$

showing that the body exhibits hyperelastic behavior during the time any particular set of parameters S_r undergoes change. Because the total work is a potential during inelastic (and elastic) processes, the incremental stiffness matrix is symmetric. Conversely, given that the stiffness matrix is symmetric when one or more S_r change, then both equations (3) and (10) follow.

If forces act on crack faces they have to be included in the set Q_j unless they are due to contact without dissipation (sliding without a shear traction or no sliding); in the latter cases, the effect of crack opening and closing may be taken into account through the form of the strain energy function. Sliding with Coulomb friction, if significant, cannot be accounted for through a work potential, and therefore the stiffness matrix is not necessarily symmetric during processes involving crack face sliding. If, however, one can use a potential to characterize the relationship between crack-face forces and relative displacements between crack faces, equation (10) may be extended to this case by including this surface potential (which may depend on additional structural parameters) in W_T. Such a simplification is applicable with surface free-energy effects (Schapery, 1990a); also, it was proposed by Schapery (1989b) to account for crack-face friction in ice under compression.

In the next section we illustrate the use of the theory by combining it with experimental results on solid propellant. One structural parameter (internal state variable) S appears to be sufficient to characterize the damage state for the particular axisymmetric loading used. For this case we may take $S = W_s$ without loss in generality. Then from

equations (3) and (4), when $S \neq 0$,

$$\frac{\partial W}{\partial S} = -1 \qquad (11)$$

and from equation (7),

$$\dot{S} \geq 0 \qquad (12)$$

3. A SPECIMEN UNDER AXIAL EXTENSION AND PRESSURE

Consider a cylindrical bar (not necessarily with a circular cross-section) which is subjected to specified axial displacement U and all-around pressure p. As generalized displacements select

$$q_1 = U/L_0 \quad , \quad q_2 = \Delta V/V_0 \qquad (13)$$

where ΔV = volume change (>0 for an increase), L_0 = initial axial length, and V_0 = initial volume. Equation (1) yields

$$Q_1 = F_1/A_0 \quad , \quad Q_2 = -p \qquad (14)$$

where F_1 is the axial force above that due to the pressure; $F_1 = 0$ when the only loading is due to p. Equations (13) and (14) are not limited to small strains. Let us now replace the generalized notation by engineering stress and strain notation, in which

$$\epsilon \equiv q_1, \quad v \equiv q_2, \quad \sigma \equiv Q_1 \qquad (15)$$

Note that v is the dilatation.

With the strain energy density $W = W(\epsilon, v, S)$, equation (2) becomes

$$\sigma = \partial W/\partial \epsilon, \quad p = -\partial W/\partial v \qquad (16)$$

Inasmuch as ϵ and p are given quantities in this example, it is helpful to rewrite the theory so that they appear as the independent variables. For this let us introduce a _dual strain energy density_ $W_d = W_d(\epsilon, p, S)$ defined by

$$W_d \equiv W + pv \qquad (17)$$

The total differential of Eq. (17) is

$$\frac{\partial W_d}{\partial \epsilon} d\epsilon + \frac{\partial W_d}{\partial p} dp + \frac{\partial W_d}{\partial S} dS$$

$$= \frac{\partial W}{\partial \epsilon} d\epsilon + \frac{\partial W}{\partial v} dv + pdv + vdp + \frac{\partial W}{\partial S} dS \qquad (18)$$

From equations (16) and (18),

$$\sigma = \partial W_d/\partial \epsilon \quad , \quad v = \partial W_d/\partial p \quad , \quad \partial W/\partial S = \partial W_d/\partial S \qquad (19a)$$

and from equation (11) when $S \neq 0$,

$$\partial W_d/\partial S = -1 \qquad (19b)$$

The total dual work is defined by

$$W_{Td} \equiv W_T + pv \qquad (20)$$

so that from equation (5),

$$W_{Td} = \int \sigma d\epsilon + \int v dp \qquad (21a)$$

and then using equation (6) and $W_s = S$,

$$W_{Td} = W_d + S \qquad (21b)$$

This reformulation of the basic theory, in which the independent variables are a mix of strain and stress variables, is covered in the more general earlier work by Schapery (1990a) using an arbitrary number of generalized forces and displacements; it is shown that W_{Td}, just as W_T, is a minimum with respect to S_m at each stable state.

Equations (19) and (21) will be used with some of the experimental data in Fig. 1 to obtain W_d, and then
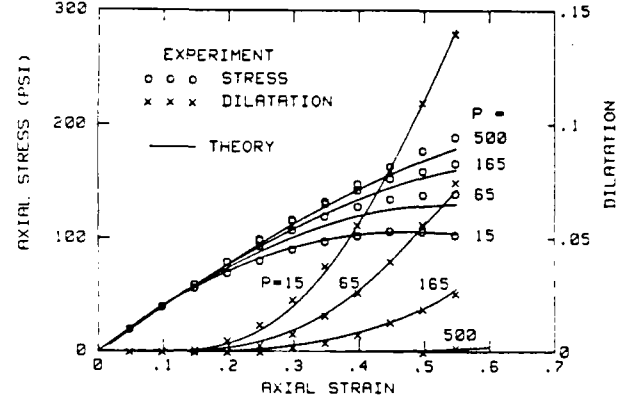

Fig. 1 Stress and dilatation behavior of a filled elastomer (65 volume percent) at four confining pressures. Experimental data from Farris (1968).

we will predict the stress and dilatation responses not used in the characterization process. In each test a constant pressure was applied and then the sample was strained at a constant rate to failure. It is to be observed that the stress-strain curves are essentially independent of pressure when the strain is sufficiently small. In the strain range for which the stress-strain curves are the same, the dilatation v is essentially zero. The dilatation in Fig. 1 is actually that due to the stress σ and does not include the very small amount due to the pressure alone. At the highest pressure there is very little dilatation, and therefore we shall assume for purposes of curve fitting that $S=0$ (undamaged material) in this case.

Determination of constitutive functions

As a start on determining W_d, let us expand it in a power series in ϵ and p and drop terms which are higher than second order,

$$W_d = c_1\epsilon + c_2 p + \frac{1}{2} c_{11}\epsilon^2 + \frac{1}{2} c_{22} p^2 + c_{12}\epsilon p \qquad (22)$$

where the coefficients are, in general, functions of S. From equation (19a),

$$\sigma = c_1 + c_{11}\epsilon + c_{12}p, \quad v = c_2 + c_{12}\epsilon + c_{22}p \qquad (23)$$

Regardless of the value of S, we assume $\sigma = v = 0$ when $\epsilon = p = 0$, and therefore $c_1 = c_2 = 0$. Equation (23) does not account for the small amount of nonlinearity in the stress-strain curve at $p = 500$. We shall account for this nonlinearity by replacing ϵ^2 in equation (22) by

$$f = f(\epsilon) \equiv \frac{2}{E} \int_0^\epsilon \sigma_s d\epsilon' \qquad (24)$$

3

where σ_5 is the stress for $p = 500$ and E is the initial slope of the stress-strain curve; note that for the linear case $\sigma_5 = E\epsilon'$, and thus $f = \epsilon^2$. Equation (22) becomes

$$W_d = \frac{1}{2} c_{11} f + \frac{1}{2} c_{22} p^2 + c_{12} \epsilon p \qquad (25)$$

Equation (19a) yields,

$$\sigma = c_{11} \frac{\sigma_5}{E} + c_{12} p , \qquad v = c_{12} \epsilon + c_{22} p \qquad (26)$$

Inasmuch as dilatation due to microcracking is never negative and there is no pressure dependence of the stress when $v=0$ (cf. Fig. 1), we set $c_{22} = c_{12} = 0$ whenever equation (26) predicts $v<0$.

The three functions of S in equation (26), i.e. c_{ij}, will be found by using the experimental data in Fig. 1 from the tests at the two lowest pressures. Specifically, we shall fit v in equation (26) to the two dilatation curves and fit σ to the stress-strain curve at the lowest pressure. However, this process gives us coefficients that depend on ϵ, not S. In order to find their dependence on S, we first solve equation (21) for S,

$$S = W_{Td} - W_d = \int_1^2 \sigma d\epsilon + \int_1^2 v dp - W_d \qquad (27)$$

where state 1 is $\epsilon = p = S = 0$ and state 2 is the current strained and pressurized state. It is assumed that equation (19b) is satisfied when $\dot{\epsilon} \geq 0$, and therefore it gives us $S = S(\epsilon, p)$. This means W_{Td} is independent of path when $\dot{\epsilon} \geq 0$, so that we may integrate between state 1 ($\epsilon=0$, $p=0$) and state 2 (ϵ, p) by going from (0,0) to (0,p) and then from (0,p) to (ϵ, p). The dilatation is (essentially) zero when $\epsilon=0$, and thus there is no contribution from the vdp term. Equation (27) becomes

$$S = \int_0^\epsilon \sigma d\epsilon' - W_d \qquad (28)$$

where σ is the stress at pressure p and strain ϵ'; hence, the integral in equation (28) is simply the area under the stress-strain curve in Fig. 1 for each pressure. The dual energy, equation (25), may be rewritten as

$$W_d = \frac{1}{2}(\sigma\epsilon + vp) + \frac{c_{11}}{2}(f - \frac{\sigma_5}{E}\epsilon) \qquad (29)$$

It is seen from equations (28) and (29) that S can be found directly from the experimental data at each pressure in Fig. 1, except for c_{11} (which depends on S). The approach we used to determine S was to start with $c_{11} = E$ in equation (29), and then find c_{11} in terms of this S, say $S^{(1)}$; an improved S, say $S^{(2)}$, was then found by using the previously derived c_{11} ($S^{(1)}$) in equation (29). Further iterations produced no further change in S and c_{11}. For each S, all three coefficients c_{11}, c_{12}, c_{22} were derived using equation (26) for two pressure levels. Namely, for pressure $p = 15$ data for both σ and v were used; introducing the subscript a, we may write for this pressure,

$$\sigma_a = c_{11} \frac{\sigma_5}{E} + c_{12} p_a, \qquad v_a = c_{12} \epsilon + c_{22} p_a \qquad (30)$$

For a second pressure, $p_b = 65$, use only v,

$$v_b = c_{12} \epsilon + c_{22} p_b \qquad (31)$$

Recall that σ_5 is a function of only ϵ, and that the coefficients are functions of only S. By neglecting

p_a in a first approximation, c_{11} and c_{12} were obtained directly from equation (30) and the data, and then they were expressed in terms of S using equation (28). Finally, equation (31) together with S for $p_b = 65$ yielded c_{22}, as $c_{12}(S)$ was known at this stage. The coefficients were recalculated by using $p_a = 15$ and the first approximations for c_{12} and c_{22} in the second terms in equation (30). Convergence was achieved with three iterations. The iterative process described earlier for S used the third approximation for c_{11} with each iteration. It is not really necessary to use iterations to find c_{ij}; we could have found all three coefficients by simultaneous solution of equations (30) and (31) with $p_a = 15$, but it would have been necessary to interpolate with respect to ϵ since the same value of S has to be used in both equations.

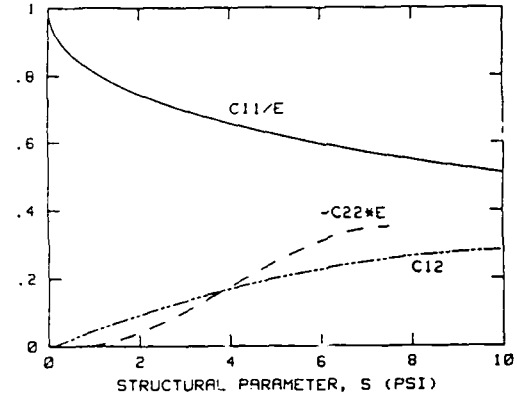Figure 2 shows the coefficients as functions of

Fig. 2   Coefficients in equation (26) for $E = 400$ psi (2.76 MPa).

the structural parameter over the S-range found from the experimental data. Low-order Chebyschev polynomials were used to obtain an analytical representation for each coefficient. Second order was used for c_{11} and c_{12} and third order was used for c_{22}; however, in the case of c_{11}, the expansion was in terms of $S^{0.48}$ instead of S.

It should be noted that the results are not limited to small strains, in that they are based on experimental data out to $\epsilon = 0.55$. However, if the geometrically linear expression for dilatation is used to calculate transverse strain ϵ_t, i.e. $2\epsilon_t + \epsilon = v$, we find the Poisson's ratio for an unpressurized bar to be simply related to c_{12},

$$v = -\epsilon_t/\epsilon = (1 - c_{12})/2 \qquad (32)$$

where $v = c_{12}\epsilon$ has been used; from Fig. 2, $v = 0.5$ at $S = 0$ and $v = 0.36$ at $S = 10$.

Prediction of the mechanical state

Having found the coefficients in W_d, equation (25), we shall now predict, S, σ, and v by means of equation (26) and the growth equation for S, equation (19b), i.e.

$$\frac{1}{2}\frac{dc_{11}}{dS} f + \frac{1}{2}\frac{dc_{22}}{dS} p^2 + \frac{dc_{12}}{dS} \epsilon p = -1 \qquad (33)$$

For each (ϵ, p) we may solve equation (33) for S by the Newton-Raphson method.

Figure 1 shows the theoretical predictions using continuous lines. Recall that the stress for $p=15$ and

dilatation for p=15 and p=65 were used in curve-fitting the coefficients. The small discrepancy between theory and experiment for these cases is due to the use of low order polynomials for c_{ij}; however, use of higher order polynomials was found to produce less smooth curves (not making a special effort to reduce the roughness) and this, in turn, lead to convergence problems in solving equation (33). Prediction of dilatation for p=165 and 500 is excellent, and the stress predictions are quite good. It should be added that the original experimental data were not available to us. Rather it was necessary to take values from the curves in Farris' (1968) publication, which is probably the main source of the difficulty in refining the curve fitting of c_{ij}.

The source of the error in stress predictions for p>15 is at least due in part to the fact that the data do not satisfy exactly the condition for existence of a work potential, regardless of the number of structural parameters which are used. This condition may be found by differentiating the two relations in equation (19a),

$$\frac{\partial v}{\partial \epsilon} = \frac{\partial \sigma}{\partial p} \qquad (34)$$

Integration yields,

$$v = \frac{\partial}{\partial p} \int_0^\epsilon \sigma d\epsilon' \qquad (35)$$

showing how dilatation can be predicted by differentiation of the area under the stress-strain curves. This relationship is not fully satisfied by the experimental data in Fig. 1; in earlier work, the existence of a work potential was explicitly checked using a less direct but equivalent relationship based on equation (16) (Farris, 1968 and Schapery, 1987b). The relative error in equation (35) is about the same as in Fig. 1 for stress predictions, and thus the latter error does not appear to be due to the use of only one structural parameter. Viscoelasticity, which is neglected here and in these earlier studies, may be at least partly responsible for the discrepancy, and thus for the difference between theory and experiment in Fig. 1; a method of accounting for viscoelasticity is discussed elsewhere (Schapery, 1990a,b).

Finally, it should be noted that Farris (1968) employed p=15 to designate atmospheric pressure, and thus used absolute pressure in characterizing the material behavior. We examined the effect of using gage pressure for p (so that the pressures in Fig. 1 are taken as 0,50,150, and 485), and found essentially the same results as shown for the theory in Figs. 1 and 2. When the characterization based on absolute pressures was used to predict the stress for p = 0, at $\epsilon = 0.55$ this stress was found to be 8 percent less than the stress for p = 15.

4. A MODEL FOR MICROCRACKING

In an earlier study (Schapery, 1986) developed a mathematical model for axisymmetric deformation behavior of a random particle-reinforced rubber (or any other relatively soft, incompressible matrix) with microcracking; changes in the microstructure were assumed to be entirely due to microcracking. Emphasis was on the micromechanics of a material which is linearly elastic for any given state of damage, although some effects of intrinsic material nonlinearity, viscoelasticity and microcrack growth were studied. Here we shall briefly describe the microstructural geometry and two different methods of

using it in predicting overall constitutive functions. The model will then be used to provide a micromechanical interpretation of the behavior discussed in Section 3 and to guide the development of a procedure that accounts for damage-induced anisotropy in more general stress states than the axisymmetric state employed in the characterization process.

For a recent evaluation of micromechanical models of linear elastic moduli without cracks, see Christensen (1990). Included is a study of the limiting behavior of composites with an incompressible matrix and a high filler volume fraction. (Solid propellant typically consists of 65-80% volume fraction of essentially rigid particles in a matrix with a Poisson's ratio very close to 0.5, and thus this limiting behavior is of interest to us.) For the so-called generalized self-consistent method (GSCM) without cracks, Christensen (1990, Table 1) gives the ratio of composite-to-matrix shear modulus as $27/16(1-v_p)^3$, where $v_p = 1$ is the particle volume fraction. For consistency with Schapery's (1986) result, the numerical factor should be 27/4 instead of 27/16; in a communication with Dr. Christensen it was confirmed that 27/4 is the correct value.

Geometry of the microstructure. Analysis methods.

In one case discussed by Schapery(1986) the random microstructure for a material like solid propellant is idealized as illustrated in Fig. 3; see
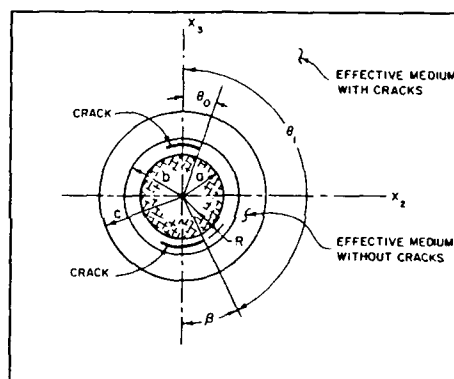

Fig. 3 Geometry for the generalized self-consistent method with microcracks.

Cornwell and Schapery (1975) and Schapery (1986) for SEM photomicrographs of solid propellant. Each particle is assumed to be rigid, spherical (with radius a), and surrounded by a incompressible rubber shell of constant thickness, b-a. A high volume fraction of filler is assumed so that $(b-a)/b<<1$. Outside of this two-phase sphere is an effective medium with the (unknown) properties of the random particle composite. One or two axisymmetric cracks are in the rubber shell; their surfaces are concentric with the particle surface, may be within the rubber or at the interface, and have sizes defined by polar angles θ_0 and θ_1.

The composite model in Fig. 3 is subjected to outer boundary displacements at r>>c which correspond to those for a uniform strain field. Namely, the displacement components u_i referred to an orthogonal set of Cartesian coordinates x_i are, for the far-field,

$$u_i = \epsilon_{ij} x_j \qquad (i,j = 1,2,3) \qquad (36)$$

where $\epsilon_{ij} = \epsilon_{ji}$ are the components of a spacewise constant strain tensor; the summation convention is used here and in what follows in that repeated indices are to be summed over their range. (This displacement representation is valid for a completely general state of small or large strains.)

In the generalized self-consistent method (GSCM) of predicting linear elastic moduli, the strain energy of the body in Fig. 3 is equated to that of a homogeneous body having the unknown effective moduli. By doing this without cracks and then with cracks, the moduli may be found from the set of equations arising from the strain energy equalities.

In the second method, the displacements in equation (36) are imposed directly on the surface r=b, and the strain energy is calculated. This energy is then equated to that for a homogeneous body with the unknown effective moduli; the equality yields expressions for finding the moduli. Without cracks, the second method provides an upper bound to the shear modulus for Hashin's (1962) composite spheres assemblage. He assumed that there is a broad enough distribution of radii b that the composite spheres fit together to form a continuum; we make the same assumption here.

Discussion of results

We have used both methods for axisymmetric straining, going beyond the work reported by Schapery (1986) and obtained the same qualitative results and similar quantitative results for the two sets of moduli, all as functions of the crack surface area. Figures 4 and 5 give the predictions of these two methods for the elastic coefficients defined by equation (26), but with σ_5/E replaced by ϵ. We used
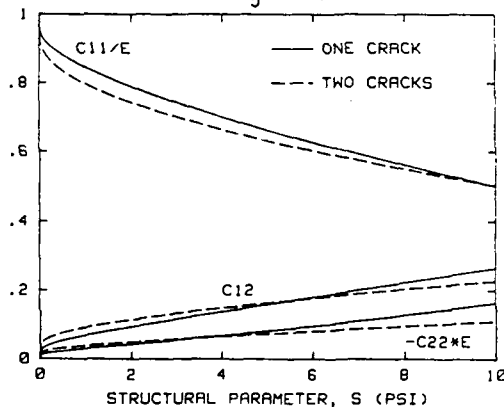
Fig. 4   Elastic coefficients from the generalized self-consistent method with c=b.
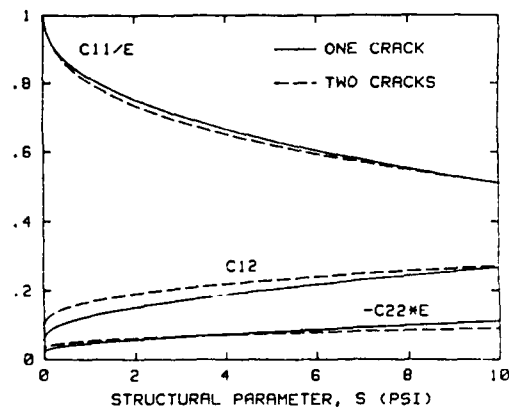
Fig. 5   Elastic coefficients from the two-phase model.

an abscissa that is proportional to the growth of surface area of the cracks in Fig. 3,

$$S = (\cos\beta_o - \cos\beta)k \qquad (37)$$

where either one crack or two equal cracks of angular size β have been used. It should be recalled that the structural parameter S used in Section 3 is the total work input/volume less the strain energy density (cf. equation (6) with $S=W_c$). In the micromechanical model, this work-difference is the work of creating new surface area. Assuming the fracture work/area is constant, $k \sim G_c$, where G_c is the (constant) critical energy release rate.

The angle β_o and factor k were selected to produce approximately the same decrease in $c_{11}(S)$ as shown in Fig. 2 for very small S and for S=10, respectively; agreement between theory and experiment for c_{11} at small S is best when β_o is vanishingly small ($\sim 10^{-8}$) for the GSCM and when $\beta_o = 0.01$ deg for the two phase model, which are the values used for Figs. 4 and 5. By definition $E = c_{11}(0)$. A study of the GSCM with $c \geq b$ showed that the closest agreement with the experimental results was achieved by using c=b (i.e. no uncracked shell around the inner two-phase cracked composite); only the latter case is shown in Fig. 4.

Consider now the prediction of stress and dilatation by means of equations (26) and (33), with $f = \epsilon^2$. The theory in Fig. 6 is in quite good
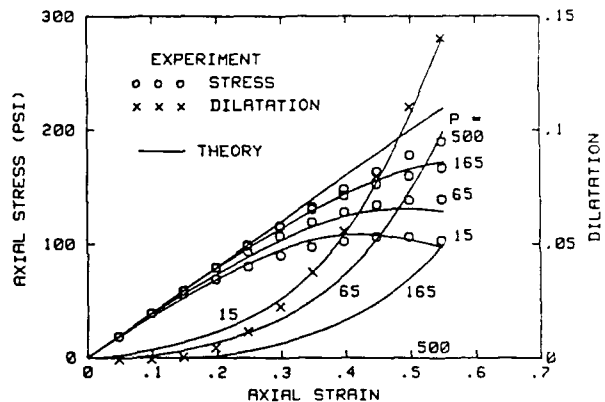
Fig. 6   Stress and dilatation prediction based on the generalized self-consistent method with two cracks.

agreement with the experimental results of Fig. 1 except for dilatation at intermediate pressures. We assumed there is no gas pressure in the cracks. Of the four cases in Fig. 4 and 5, the GSCM with two cracks agrees best with experimental data. The two-phase model results, Fig. 5, lead to the poorest prediction because of the poor behavior of c_{12} and dc_{11}/dS, especially at small values of S. For all four theoretical cases, the magnitude of the coefficient c_{22} is well below the experimental result in Fig. 2. Consequently, the dependence of dilatation on pressure is not accurately predicted. Referring to equation (26), it is seen that c_{22} is a plane-strain bulk compliance in that $c_{22} = v/p$ for $\epsilon=0$.

Let us now return to equation (37) and the results for the two-crack GSCM in order to relate k to G_c and estimate the value of G_c. The surface area for two equal-length cracks at a mean radius R is

$$A = 4\pi R^2(1-\cos \beta) \qquad (38)$$

The volume of the representative volume element (the two-phase core in Fig. 3) is approximately $4\pi R^3/3$ if $(b-a)/b \ll 1$, and therefore the fracture work/volume

6

is

$$S = 3(\cos\beta_0 - \cos\beta)G_c/R \qquad (39)$$

Showing that $k = 3G_c/R$. The value of $k = 226$ psi provides the best agreement between theory and experiment for c_{11} at $S = 10$, and was used in predicting the stress and dilatation curves in Fig. 6; the predictions depend on dc_{11}/dS through equation (33), which could have lead to an optimum k that is different from that for c_{11} alone. (There is also weak dependence on the other coefficients and their derivatives since $p\ne 0$). For $k = 226$ psi as well as $\beta = 0$ and a representative radius for particles in solid propellant of $R = 10^{-3}$in (25μm), we find $G_c = 0.08$ lb/in (13 J/m^2). The matrix in the composite studied here is polyurethane rubber; it is encouraging that the intrinsic or threshold value of G_c is 0.05 lb/in for an unfilled polyurethane rubber studied previously (Schapery, 1975). Finally, we note that $\beta = 22$ deg at $\epsilon = 0.55$ for the predictions in Fig. 6 when $p=15$; for the case of one crack $\beta = 37$ deg. When $p>15$ the maximum crack angles are smaller.

Although the damaged material is transversely isotropic, it is of interest to compare the c_{ij} to those for a fully isotropic material. We find in the latter case

$$c_{11}= E, \qquad c_{12}= 1-2\nu,$$
$$\qquad (40)$$
$$-Ec_{22}= 2(1-2\nu)(1+\nu) = 3c_{12}-c_{12}^2$$

Observe that $c_{12}= 0.28$ at $S=10$ in Fig. 2, which implies for an isotropic material $-c_{22}E = 0.76$; moreover, $-Ec_{22}/c_{12}= 3$ at $c_{12} = 1$. Both experimental (Fig. 2) and theoretical results (Figs. 4 and 5) show that the plane strain bulk compliance c_{22} is considerably less than that for an isotropic material. This behavior is consistent with what one expects physically because the dominant orientation of microcrack normals is in the direction of axial stretching. However, the microcrack model, in which all cracks have an axis of symmetry in the axial straining direction, exhibits even greater anisotropy than the experimental results. It is likely that an improvement in the model would be gained by allowing for a distribution of orientations θ of the crack symmetry axis x_3 relative to the global material axis x_3, Fig. 7. This approach was outlined previously for the two-phase model (Schapery, 1987a) and could be implemented using the GSCM; in the latter case, two-phase cores with different orientations would be
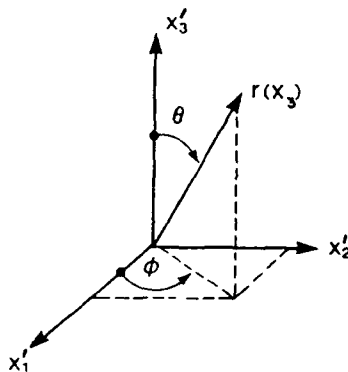

Fig. 7 Coordinate systems.

embedded in an effective medium. It would be necessary to account for locally nonaxisymmetric loading on each two-phase core (cf. equation 41)). Another generalization that should yield improved values of the plane strain bulk compliance is the introduction of matrix compressibility. Whether or not the latter generalization alone would be sufficient to obtain realistic values of c_{22}, at least for overall axisymmetric loading, is not yet known.

Crack initiation and early growth behavior

The predictions made so far in this section are based on the assumption that there are either two equal cracks or one crack in the matrix layer around each particle prior to loading; but they are very short ($\beta \le 0.01$ deg) prior to loading. We have also studied the case of two, initially unequal cracks. With axial straining it was found that the energy release rate of the shortest crack reached the critical value first and that only it grows until it reaches the size of the initially largest crack; without cracks the highest stresses are at the top and bottom of the particle in Fig. 3. Then, with further straining, both grow as a pair of equal, stable cracks. Thus, when two very short cracks pre-exist, the only situation of practical interest for most of the available straining range is that of two equal-size cracks.

The "pre-existing" cracks may be indeed that, arising during processing. Most, however, probably develop from the high triaxial tensile stress concentrations between particles. Early experimental and theoretical work by Gent and Lindley (1959) showed that the strength of unfilled rubber in equal triaxial tension is approximately $5E_r/6$, where E_r is the Young's modulus (at zero strain) of the rubber. This value was predicted by considering the growth of an initial, arbitrarily small, spherical void due to remote, equal triaxial tension. When the tension reaches and then exceeds $5E_r/6$ the void is predicted to become unstable (due to a geometric nonlinearity) and grow without bound. As hypothesized by Williams and Schapery (1965), when the stress $5E_r/6$ is approached a Saturn-ring crack forms and then grows (until there is sufficient local stress relief for arrest). The smaller the initial cavity is, the closer the strength is to $5E_m/6$; for cavities on the order of 10μm or less we estimate for the material studied above that the strength is close to this value.

Recent work by Gent and Wang (1990) shows that the triaxial strength of rubber is somewhat above this value when the size of the cavity is extremely small. The new prediction accounts better than previously for the high-strain behavior of rubber; it is believed there is an error in the energy analysis, stemming from the use of internal cavity pressure (instead of external tension) which acts on the fracture surface, but the general conclusions appear to be correct. Considering the very high stress in a real highly-filled composite propellant with irregularly-shaped particles, it is reasonable to view the "pre-existing" cracks in the above analysis as the arrested Saturn-ring cracks. That the experimentally observed dilatation is less than the prediction (Fig. 6) at small strains may be, at least in part, due to the lack of initial cracks until the critical stress with a value of approximately E_r between particles is reached.

5. GENERALIZATIONS FOR ARBITRARY STRAIN STATES

Axisymmetric damage

With axisymmetric damage the composite material is transversely isotropic. Regardless of the micromechanical model employed, one may show that the strain energy density in this case for a linearly elastic material can always be written in the form

$$W_0 = \frac{1}{2} [A_{11}v^2 + A_{22}e_d^2 + 2A_{12}e_d v + A_{44}(\gamma_{13}^2 + \gamma_{23}^2)$$

$$+ A_{66}(\gamma_{12}^2 + e_s^2)] \qquad (41)$$

where x_3 is the axis of material symmetry and

$$e_s = \epsilon_{22} - \epsilon_{11} , \qquad e_d = \epsilon_{33} - v/3$$

$$v = \epsilon_{11} + \epsilon_{22} + \epsilon_{33} , \qquad \gamma_{12} = 2\epsilon_{12} \qquad (42)$$

$$\gamma_{23} = 2\epsilon_{23} , \qquad \gamma_{13} = 2\epsilon_{13}$$

and the five coefficients A_{ij} are elastic moduli (which depend on the state of cracking or damage). The strains ϵ_{ij} are the tensor components introduced in equation (36).

The work-conjugate stresses are

$$\sigma_v = \partial W_0/\partial v = A_{11}v + A_{12}e_d$$

$$\sigma_d = \partial W_0/\partial e_d = A_{12}v + A_{22}e_d$$

$$\sigma_s = \partial W_0/\partial e_s = A_{66}e_s$$

$$\tau_{12} = \partial W_0/\partial \gamma_{12} = A_{66}\gamma_{12} \qquad (43)$$

$$\tau_{13} = \partial W_0/\partial \gamma_{13} = A_{44}\gamma_{13}$$

$$\tau_{23} = \partial W_0/\partial \gamma_{23} = A_{44}\gamma_{23}$$

The virtual work condition $\delta W' = \sigma_{ij}\delta\epsilon_{ij}$, for each (i,j) pair, yields

$$\sigma_v = \frac{1}{3}(\sigma_{11} + \sigma_{22} + \sigma_{33})$$

$$\sigma_d = \sigma_{33} - (\sigma_{11} + \sigma_{22})/2 \qquad (44)$$

$$\sigma_s = (\sigma_{22} - \sigma_{11})/2$$

where σ_{ij} are the components of the stress tensor in the x_i coordinate system. For an isotropic material

$$A_{11} = K , \qquad A_{22} = 3G , \qquad A_{12} = 0$$
$$A_{44} = A_{66} = G \qquad (45)$$

where K and G are the bulk modulus and shear modulus, respectively,

$$K = E/3(1-2v) , \qquad G = E/2(1+v) \qquad (46)$$

In deriving moduli for the micromechanical models based on the geometry in Fig. 3, we found the form of W_0 and the associated strains in equations (41) and (42) to be especially convenient. It was the A_{ij} in these equations that were developed first using the two methods discussed in Section 4. Then, by relating the strains and stresses in equations (42) and (44) to those in equation (26) (with $\sigma_E/E = \epsilon$), we obtained the c_{ij}. For reference, the relationships are

$$c_{11} = (A_{12}^2 - A_{11}A_{22})c_{22}$$

$$c_{12} = (A_{12} - A_{22}/3)c_{22} \qquad (47)$$

$$c_{22} = (2A_{12}/3 - A_{11} - A_{22}/9)^{-1}$$

The use of A_{ij} in the micromechanical model not only simplifies the analysis, but provides some moduli which are practically independent of damage over the range studied in Section 4. Namely, as β increased from zero to its maximum value at the strain of 0.55, we found A_{11}/E decreased smoothly from infinity to about unity, while A_{12} and A_{44} decreased by about 25 and 15 percent, respectively. The remaining two coefficients, A_{22} and A_{66}, changed by 7 percent at most. This result implies the energy release rate for each crack in a two-crack composite core,

$$ERR = -\frac{4}{3}\pi b^3 \frac{\partial W_0}{\partial(\text{crack area})} = -\frac{R}{3\sin\beta}\frac{\partial W_0}{\partial \beta} \qquad (48)$$

is dominated by $dA_{11}/d\beta$ unless the dilatation is very small relative to the other strains. Thus

$$ERR = -\frac{Rv^2}{6\sin\beta}\frac{dA_{11}}{d\beta} \qquad (49)$$

The crack growth condition is $ERR = G_c$; this equation implies β depends mainly on a scalar invariant, the dilatation. We may therefore consider the dilatation to be at least a rough measure of the magnitude of damage during loading; we have verified this numerically using both methods in Section 4 for the case of a specimen loaded by axial straining and pressure. Now, as A_{11} scales with E, the initial Young's modulus, we may write for $\dot{v} \geq 0$,

$$\beta = \text{function}(REv^2/G_c) \qquad (50)$$

which is an increasing function of the argument; when $\dot{v} < 0$, the condition of constant damage, $\dot{\beta} = 0$, should be used unless significant healing occurs.

Regardless of whether only $dA_{11}/d\beta$ or the other modulus derivatives as well are needed in equation (48), the material parameters affect the damage through one dimensionless ratio, RE/G_c. A decrease in radius R or an increase in G_c reduces the amount of damage.

The strain energy density W_0 in equation (48) is considered to be that for a composite with many particles, each with two cracks in the example used. As both W_0V_0 and the total crack surface area are proportional to the number of particles, there is no effect of this number on ERR. Similarly, the work/volume in equation (39) is independent of the number of particles. However, both equations exhibit dependence on the radius R. With a distribution of sizes, this radius has to be interpreted as an "effective" value for the simplified models employed. If one wants to explicitly account for two or more different sizes, say $R_m(m=1,2,...)$, they have to be explicitly included by using two or more two-phase composite cores (particle plus rubber layer) in the effective modulus analysis. Growth of each of the associated crack angles β_m obeys equation (48), with $ERR = G_c$. Each angle β_m, or the associated crack area A_m, is the structural parameter S_m of Section 2 which obeys equation (3); if area is used, $f_m = (ERR)_m$. However, according to approximate equation (50) for

each m, all angles depend primarily on one quantity, the maximum dilatation v_{max}. This maximum value is the current value of dilation if $\dot{v} > 0$ for the entire loading history. Thus there is only one significant structural parameter S; we may use as this parameter the maximum dilatation, the total fracture work W_S for all cracks (as in Section 2), or any other quantity which is related in a one-to-one fashion to W_S. If, however, v_{max} is used the total work W_T will exhibit some path-dependence when $\dot{v} < 0$ because equation (50) is not exact. Therefore, it is better to use $S = W_S$ since this choice guarantees path-independence of work when $\dot{S} < 0$.

In some cases the damage may be axisymmetric even if the loading is not. Suppose, for example, $\epsilon_{11} = \epsilon_{22}$ when $\epsilon_{33} > (\epsilon_{11}, \epsilon_{22})$ and all shear strains vanish. Then, if ϵ_{33} alone determines the damage orientation, it will be axisymmetric. In such a case the experimental results in Section 3 can be used directly to derive A_{11}, A_{22}, and A_{12}, without a micromechanical model. The remaining shear moduli A_{44} and A_{66} have been found from the model to be insensitive to damage, and thus we may use for them the shear modulus in the undamaged state. This approach has been used to predict behavior in simple shear from the results in Fig. 2 (Schapery, 1987a).

In general, the axis of isotropy (x_3 in Fig. 3) may not be parallel to an axis in the coordinate system used to represent the overall (applied) strains. In order to allow for an arbitrary orientation use

$$u'_j = \epsilon'_{ij} x'_j \tag{51}$$

where ϵ'_{ij} are the applied strains referred to conveniently defined coordinates x'_i. The relationship between the strains in equations (42) and (51) is of course given by the second-order tensor transformation

$$\epsilon_{ij} = m_{ik} m_{jn} \epsilon'_{kn} \tag{52}$$

where m_{ij} is the cosine of the angle between the x_i and x'_j axes. Substitution of equation (52) into (42) gives us W_0 in terms of ϵ'_{ij}.

Nonaxisymmetric damage

For a general state of overall stress and strain, referred to the x'_i coordinates,

$$\sigma'_{ij} = B'_{ijk\ell} \epsilon'_{k\ell} \tag{53}$$

If the damage is axisymmetric and we use $x'_i = x_i$, the associated moduli $B_{ijk\ell}$ may be easily expressed in terms of the five A_{ij} in equation (43). As $B'_{ijk\ell}$ is a fourth-order tensor, we may then predict it for any orientation of x'_i. Both the GSCM and two-phase model discussed in Section 4 can be used to predict $B'_{ijk\ell}$ with nonaxisymmetric damage. It may be acceptable to assume each crack is axisymmetric (thus simplifying the two-phase core analysis) as long as one includes cores with different symmetry axis orientations v_m, ϵ_m (cf. Fig. 7). If the second method of Section 4 is used, which is based on the two-phase composite ($r < b$), the global strain energy density will consist of a sum of strain energies, each having the form of equation (41), but with the strains ϵ_{ij} expressed in terms of ϵ'_{ij} and the axis orientation through equation (52). The W_0 for the two-phase core in the GSCM is similar to that in equation (41), but is expressed in terms of local boundary displacements instead of the overall strains (Schapery, 1986).

If an overall strain history is imposed for which

the orientation of the maximum principal strain is not fixed, one will have to include composite core orientations that reflect this history. Suppose, for example, the principal strain orientations do not change, but at one time or another each principal strain has the largest value and it is large enough to produce a family of cracks. In general, the composite will be orthotropic, and the moduli will depend on at least three structural parameters, one b (or S) for each principal direction. The two-phase core in Fig. 3 is simple enough that one can predict the crack face displacements, and thus readily introduce constraints which prevent crack-face overlap when necessary.

Different types of damage may be introduced. If the loading is like that discussed in Section 3, but the axial strain is compressive instead of tensile, the damage will be axisymmetric, but the crack axis will be normal to the straining axis. A reasonable description for this damage may be a belt-like crack that encircles the particle about the vertical axis. The strain energy density of a composite core with such a crack can be easily derived using the previously developed perturbation solution (Schapery, 1986).

CONCLUSIONS

A thermodynamically based theory of mechanical state behavior with damage growth was reviewed and then successfully applied to a filled rubber under axisymmetric loading. The analysis proved to be quite simple because of the path-independence of work (the work potential) and the requirement of only one structural parameter (or internal state variable).

Two different micromechanical models were then used to relate overall composite behavior to microcracking and associated material parameters, including filler size; the amount of damage is a function of these parameters through one dimensionless ratio, RE/G_c, where R is a characteristic particle size, E is the initial Young's modulus, and G_c is the critical energy release rate for microcracks. The model based on the generalized self-consistent method (GSCM), which is a special case of the thermodynamic theory, agrees best with the experimental results.

In view of these encouraging results, it is believed desirable to extend the GSCM to predict damage orientation and growth as well as overall mechanical behavior under general strain states. With damage localization, such as the growth of a macrocrack in the damaged continuum, the theory should still apply except where there are high strain gradients, such as near the macrocrack edge. Then, as long as the work potential theory is applicable to the continuum, the J integral will be applicable as a macrocrack characterizing parameter in many cases (Schapery, 1987b). Viscoelastic effects may be easily incorporated in the theory using approximations described elsewhere (Schapery, 1990b).

REFERENCES

Christensen, R.M., 1990, "A Critical Evaluation for a Class of Micromechanics Models," Journal of the Mechanics and Physics of Solids, Vol. 38, pp. 379-404.

Cornwell, L.R. and Schapery, R.A., 1975, "SEM Study of Microcracking in Strained Solid Propellant," Metallography, Vol. 8, pp. 445-452.

Farris, R.J., 1968, "The Character of the Stress-Strain Function for Highly Filled Elastomers," Transactions of the Society of Rheology, Vol. 12:2, pp. 303-314.

Gent, A.N. and Lindley, P.B., 1959, "Internal Rupture of Bonded Rubber Cylinders in Tension," Proceedings of the Royal Society A, Vol. 249, p. 195

Gent, A.N. and Wang, C., 1990, "Fracture Mechanics and Cavitation in Rubberlike Solids," Journal of Materials Science, in press. Also published as a University of Akron report.

Hashin, Z., 1962, "The Elastic Moduli of Heterogeneous Materials," Journal of Applied Mechanics, Vol. 29, pp. 143-150.

Krajcinovic, D. and Lemaitre, J., 1987, Continuum Damage Mechanics, Theory and Applications, Springer-Verlag, New York-Wien.

Mullins, L., 1969, "Softening of Rubber by Deformation," Rubber Chemistry Technology, Vol. 42, pp. 339-362.

Schapery, R.A., 1975, "A Theory of Crack Initiation and Growth in Viscoelastic Media III," International Journal of Fracture, Vol. 11, pp. 549-562.

Schapery, R.A., 1982, "Models for Damage Growth and Fracture in Nonlinear Viscoelastic Particulate Composites," Proceedings, Ninth U.S. National Congress of Applied Mechanics, The American Society of Mechanical Engineers, Book No. H00228, p. 237-245.

Schapery, R.A., 1986, "A Micromechanical Model for Nonlinear Viscoelastic Behavior of Particle-Reinforced Rubber With Distributed Damage," Engineering Fracture Mechanics, Vol. 25, pp. 845-867.

Schapery, R.A., 1987a, "Nonlinear Constitutive Equations for Solid Propellant Based on a Work Potential and Micromechanical Model," Proceedings, 1987 JANNAF Structures and Mechanical Behavior Subcommittee Meeting, CPIA. Also Texas A&M Report MM 5456-87-4.

Schapery, R.A., 1987b, "Deformation and Fracture Characterization of Inelastic Composite Materials Using Potentials," Polymer Engineering and Science, Vol. 27, pp. 63-76.

Schapery, R.A., 1989a, "Mechanical Characterization and Analysis of Inelastic Composite Laminates with Growing Damage," Mechanics of Composite Materials and Structures, AMD-Vol. 100, The American Society of Mechanical Engineers, pp. 1-9.

Schapery, R.A., 1989b, "Models for the Deformation Behavior of Viscoelastic Media with Distributed Damage and Their Applicability to Ice," Proceedings, IUTAM/IAHR Symposium on Ice/Structure Interaction, St. John's, Newfoundland, August 1989, in press.

Schapery, R.A., 1990a, "A Theory of Mechanical Behavior of Elastic Media with Growing Damage and Other Changes in Structure," Journal of the Mechanics and Physics of Solids, Vol. 38, pp. 215-253.

Schapery, R.A., 1990b, "Simplifications in the Behavior of Viscoelastic Composites with Growing Damage," Proceedings, IUTAM Symposium on Inelastic Deformation of Composite Materials, May 29-June 1, 1990, in press. Also published as Texas A&M Report No. 27010-90-8.

Swanson, S.R., 1983, "A Constitutive Formulation for High-Elongation Propellants," J. Spacecraft and Rockets, Vol. 20, p. 559

Williams, M.L. and Schapery, R.A., 1965, "Spherical Flaw Instability in Hydrostatic Tension," International Journal of Fracture, Vol. 1, pp. 64-72.